Mildred S. Dresselhaus *
John G. Mavroides *

The Fermi Surface of Graphite

Abstract: Recent magnetoreflection measurements in pyrolytic graphite have been interpreted using the magnetic energy levels obtained from the McClure-Inoue secular equation and the appropriate selection rules for interband transitions. Combining these results with those of the de Haas - van Alphen effect, the band parameters of the Slonczewski-Weiss model have been evaluated and the Fermi surface determined. The magnetoreflection experiment indicates considerable warping of the Fermi surface, particularly for holes. Further experiments to determine this warping more precisely are discussed.

The magnetoreflection technique has been recently applied to study the electronic band structure of graphite.[1] Whereas, previously, at best only a few of the band parameters of graphite have been determined[2] in a single experiment, the magnetoreflection results have provided a quantitative evaluation of most of the band parameters of the Slonczewski-Weiss model in a single experiment. For some of these band parameters, e.g. γ_3, γ_4 and Δ using the notation of Ref. 2, quantitative values are now available for the first time. With these new values of the band parameters, the shape of the Fermi surface given by McClure[3] and Nozières[4] was re-examined in a more quantitative fashion.

The magnetic field dependence of the optical reflectivity was measured on the best available pyrolytic graphite samples,† which were mounted with the trigonal face exposed. The light beam was almost normally incident to this trigonal plane and the static magnetic field was directed along the trigonal axis. A typical recorder trace is shown in Fig. 1 for photon energy $\hbar\omega = 0.0945$ eV and $T \cong 4°$K. The oscillatory magnetic field dependence of the reflectivity is attributed to interband transitions between quantized magnetic energy levels. The analysis of the dependence of these oscillations on photon energy and magnetic field provides us with a determination[1] of the band parameters Δ, γ_0, γ_1, γ_3 and γ_4.

Although these measurements were carried out on pyrolytic graphite, there is reason to believe that the band parameters determined in the magnetoreflection experiment are closely related to the actual band parameters of single-crystal graphite. The pyrolytic graphite samples used in the magnetoreflection experiment were heat treated at 3600°C and one of these samples was prepared at the same time and in the same manner as the samples used in the resistivity and magnetoresistance measurements of Klein, Straub and Diefendorf.[5] Such highly stress-annealed pyrolytic graphite has been shown to exhibit essentially single-crystal characteristics with regard to carrier mobility, carrier concentration and diamagnetic susceptibility.[5]

In the magnetoreflection experiment, magnetic fields above 10 kG restrict the electronic motion in the basal plane to cyclotron orbits of radius <1000 Å. There is evidence that the mean free path for motion in the basal plane is much larger than the cyclotron radius and is limited not by boundary scattering of the crystallites but rather by impurity and thermal scattering of the lattice. Magnetoreflection oscillations in the best pyrolytic graphite material are observed even at room temperature, but the line width of the oscillations decreases rapidly as the temperature is lowered. A mean free path of $l \gtrsim 1\mu$ is estimated from the line width of the oscillations at liquid helium temperature, and this value is consistent with the mobility determination of Klein, Straub and Diefendorf.[5] The electronic motion in the trigonal direction is limited by microcracks, which are spaced approximately 1 μ apart.[6] The magnetoreflection experiment is sensitive only to electrons moving in the infrared skin depth, which is also ~ 1 μ. Increasing the degree of crystalline perfection of the pyrolytic graphite not only increases the amplitude

* Lincoln Laboratory, Massachusetts Institute of Technology. (Lincoln Laboratory is operated with support from the U. S. Air Force.)
† We are grateful to Dr. R. J. Diefendorf of the General Electric Research Laboratory for kindly supplying us with several pyrolytic graphite samples.

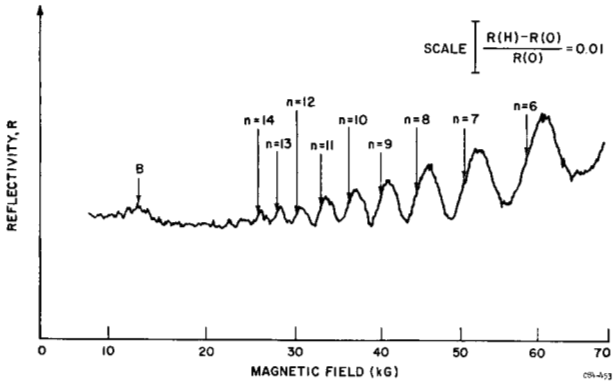

Figure 1 **Experimental traces of the oscillatory reflectivity of a pyrolytic graphite sample in a magnetic field.** *Photons of energy 0.0945 eV are incident along the trigonal axis, which is parallel to the magnetic field. The scale for the differential reflectivity is indicated. Interband transitions associated with point* K *of the Brillouin zone are indicated by n = integer. One member of the series associated with point* H *is indicated by* B.

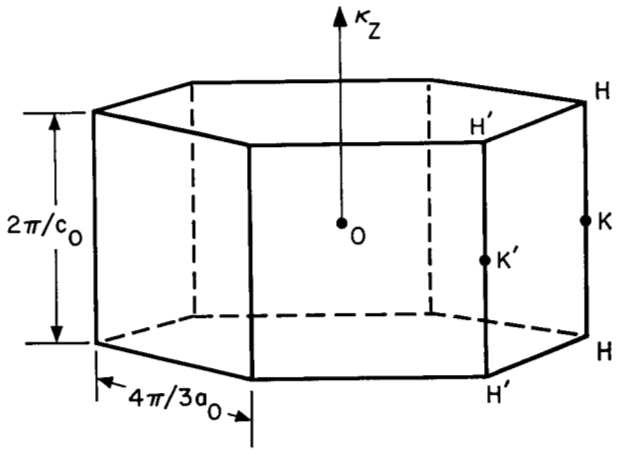

Figure 2 **Brillouin zone for 3-dimensional graphite.** *The quantities a_0 and c_0 are, respectively, the magnitudes of the primitive lattice vectors in and perpendicular to the layer plane. The Fermi level is located in the vicinity of the edges* HKH *and* H'K'H'.

of the magnetoreflection oscillations but also slightly changes the periodicity of the oscillations; the more perfect the pyrolytic graphite, the more closely its band parameters approach the single-crystal values. The values of the band parameters given in this paper were determined from measurements on a sample similar to those used by Klein, Straub and Diefendorf.[5]

As is shown in Fig. 1, two types of oscillations are observed in a typical magnetoreflection recorder trace. There is a series of sharp, closely spaced oscillations which are associated with interband transitions between the two E_3 bands in the vicinity of point K in the Brillouin zone of Fig. 2. In addition, a second series of broader, more widely spaced oscillations are found, these being associated with interband transitions between the degenerate E_3 bands and the degenerate E_1 and E_2 bands located in the vicinity of point H in the Brillouin zone. Figure 3b illustrates the dependence of the energy $E(\xi)$ of the four π bands on crystal momentum along the Brillouin zone edge HK, according to the band structure model of Slonczewski and Weiss.[2] The dimensionless wave vector is defined as $\xi = \kappa_z c_0/2\pi$. The location of the Fermi energy is indicated by a dashed line, which encloses pockets of holes and electrons in the vicinity of points K and H, respectively. As we move in a layer plane away from the edge at points K and H and towards the center of the Brillouin zone, the dependence of $E(\sigma)$ on σ assumes the form given in Figs. 3 a and 3c, respectively, in which the dimensionless wave vector measured from the zone edge is used, $\sigma = \frac{1}{2}\sqrt{3}a_0\,|\kappa|$. We note that the two E_3 bands are degenerate only along the edges HKH and H'K'H' and the bounding planes $\kappa_z = \pm\,\pi/c_0$, while bands E_1 and E_2 are degenerate only in these bounding planes. When a magnetic field is applied along the trigonal direction, each of the four π bands shown in Fig. 3b splits into quantized

Figure 3 **Dependence of the energy of the π bands on wave vector, according to the band structure model of Slonczewski and Weiss.** (*a*) *Energy, $E(\sigma)$, versus dimensionless wave vector σ in the layer plane for $\kappa_z = 0$ (i.e. about point* K). (*b*) *Energy, $E(\xi)$, versus dimensionless wave vector ξ along the edges* HKH *or* H'K'H'. (*c*) *$E(\sigma)$ versus σ in the layer plane for $\kappa_z = \pi/c_0$ (about point* H).

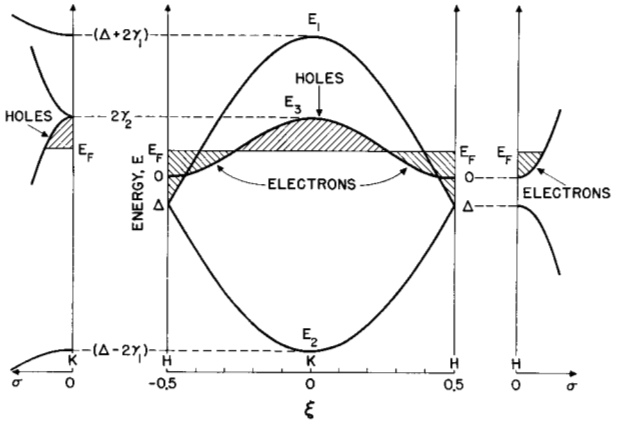

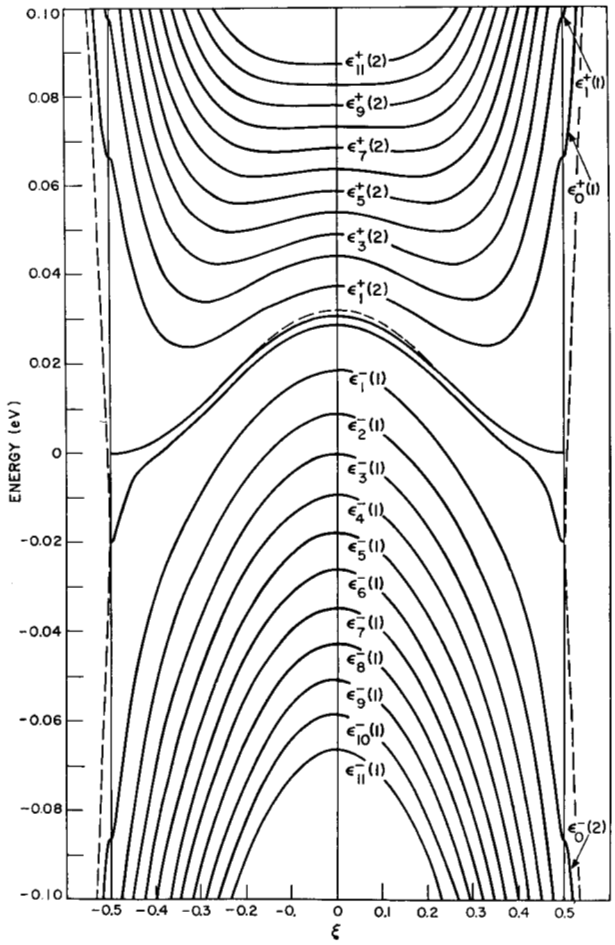

Figure 4 **Magnetic energy contours at 50 kG for the four π bands in graphite calculated from solution of the McClure-Inoue equation for the band parameters determined by experiment.** *The Inoue notation is used to label the levels. The band edges ($H = 0$) are indicated by dashed curves.*

harmonic oscillator type levels, which are solutions of the McClure-Inoue determinantal equation[7] and are labeled by the quantum number l. The resulting magnetic energy levels at $H = 50$ kG are given in Fig. 4 for the band parameters deduced from experiment. The two groups of magnetic levels which are involved in the interband transitions about point K, and associated with the two E_3 bands of Fig. 3b, are represented in the region $-0.5 < \xi < 0.5$. As ξ increases, approaching point H, the bands E_3 and E_1 of Fig. 3b intersect. Interband transitions near point H occur from the degenerate E_1, E_2 levels to the degenerate E_3 levels, illustrated in the extended zone scheme of Fig. 4 for $|\xi| > 0.5$. Interband transitions at point H obey the selection rules $\Delta l = \pm 1$. The resonant frequency for oscillations in this series at low and high magnetic fields are determined by the parameters Δ and γ_0, respectively. Interband transitions at point K also obey the same selection rules, but now applied to the two E_3 bands. In the limit of high photon energies, the magnetic energy contours about point K approach simple, parabolic, equally spaced levels. For fixed values of Δ and γ_0, interband transitions in this limit are most sensitive to the parameter γ_1, (γ_1/γ_0^2) being proportional to the reduced effective mass. In the low photon energy limit, the unequal spacing of the energy levels for low quantum numbers allows the evaluation of the band parameters γ_3 and γ_4, and to a lesser extent γ_5. The exact values of γ_3 and γ_4 depend upon the magnitudes assigned to γ_0, γ_1 and Δ, while the evaluation of γ_5 is influenced by the values assigned to all the other parameters.

The magnetoreflection experiment, in principle, is also sensitive to γ_2 but only in the limit of very low photon energies, appropriate to the observation of *intraband* transitions. Since the photon energies available with our experimental setup were much too high for the observation of de Haas - van Alphen type oscillations, we have evaluated γ_2 from the results of the oscillatory diamagnetic susceptibility[8] and magnetoresistance measurements.[9] A summary of the band parameters obtained from experimental data is given in Table 1. Using these values of the band parameters a quantitative determination of the Fermi surface was carried out.

The Fermi energy E_F is determined by the requirement that the number of holes be equal to the number of electrons. The hole density, n_h, is given by the unoccupied volume of the first Brillouin zone, or

$$n_h = \frac{1}{4\pi^3} \int_{B.Z.} [1 - f_0(E)]\, d^3\mathbf{k}. \tag{1}$$

This small unoccupied volume is located near the edges HKH and H′K′H′ and is bounded by the energy surface $E = \epsilon^-(1)$ and the Fermi surface $E = E_F$. (Figs. 3 and 4). It is convenient to choose the origin of the coordinate system at point K and to integrate over a cylinder just large enough to contain all the holes. By symmetry there are exactly two such complete cylinders with axes along the κ_z direction. The volume in the Brillouin zone associated with the electron carriers is bounded by the energy surfaces $E = \epsilon^+(2)$ and $E = E_F$, and the electron concentration is given by an expression obtained from Eq. (1) by replacing $[1 - f_0(E)]$ by $f_0(E)$. There is also a small pocket of minority electron carriers near points H and H′, bounded by the energy surfaces $E = \epsilon^+(1)$ and $E = E_F$. The density of these carriers is found in the same manner.

The numerical calculation of the integrals such as in Eq. (1) was carried out on an IBM 7094 computer. In the limit $\gamma_3 = 0$, these integrals can be evaluated exactly, since in this case the cross sectional areas of the Fermi surface exhibit no angular variation. This is, in fact, the

Table 1 **Band parameters for graphite.**

Band parameters	Present work		Other recent determinations	
	Values, eV	*Method of determination**	*Values, eV*	*Reference*
γ_0	2.88	MR, high field, point H	2.8	7
γ_1	0.395	MR, high quantum levels, point K	0.27	10
γ_2	0.016	DH VA periods	0.017	10
γ_3	0.145	MR, low quantum levels, point K	$\sim$0.13	11
γ_4	−0.20	MR, low quantum levels, point K†	$\sim$0.28	12
γ_5	0.016	$\gamma_5 = \gamma_2$	$\gamma_5 = \gamma_2$	7
Δ	−0.02	MR, low field, point H	−0.10	12
E_F	0.019	number of holes = number of electrons	0.02	3

*MR ≡ Magnetoreflection
DH VA ≡ de Haas-van Alphen

† The sign of γ_4 is chosen to be consistent with the ratio of the DH VA periods.

limit which was originally treated by McClure.[3] In reality, $\gamma_3 \neq 0$, and the integrals of Eq. (1) can be evaluated only approximately.

The two cylinders in the Brillouin zone are each sliced perpendicular to the trigonal axis to form t thin discs, each of height $\Delta\xi = 1/t$, and occupied volume = $A\,\Delta\xi$, in which A is the occupied cross sectional area at the median height of the disc. This area A can be evaluated exactly in almost all cases. Those few discs having occupied cross sectional areas for which the radius vector is a multivalued function of angle were evaluated approximately by a logical routine. In this case, the discs were further subdivided into a sufficiently large number of small cells of equal volume, and the occupancy of each cell was tested. The occupancy of a cell is determined by solving the 4 × 4 Hamiltonian of the Slonczewski-Weiss theory for the coordinates at the center of the cell and by then comparing this energy to the Fermi energy. This same 4 × 4 Hamiltonian is also solved when the occupied cross sectional area is computed directly.

It has been observed by McClure[3] and shown explicitly in the present work that γ_3 has only a small effect on the cross sectional areas, on the Fermi level and on the carrier density. On the other hand, the effect of γ_3 on the shape of the Fermi surface is considerable. A model of the Fermi surface for holes and electrons (both majority and minority) is shown in Fig. 5. This figure is a generalization of the Fermi surface previously given by McClure.[3] The orbit at $\xi = 0$ encloses the extremal de Haas - van Alphen hole area and exhibits relatively large fluting as can be seen in the scale drawing of Fig. 6. The maximum radius of this cross section is only 1.2% of the distance from point K to the center of the Brillouin zone. As ξ increases, the warping becomes more marked, as is shown in the

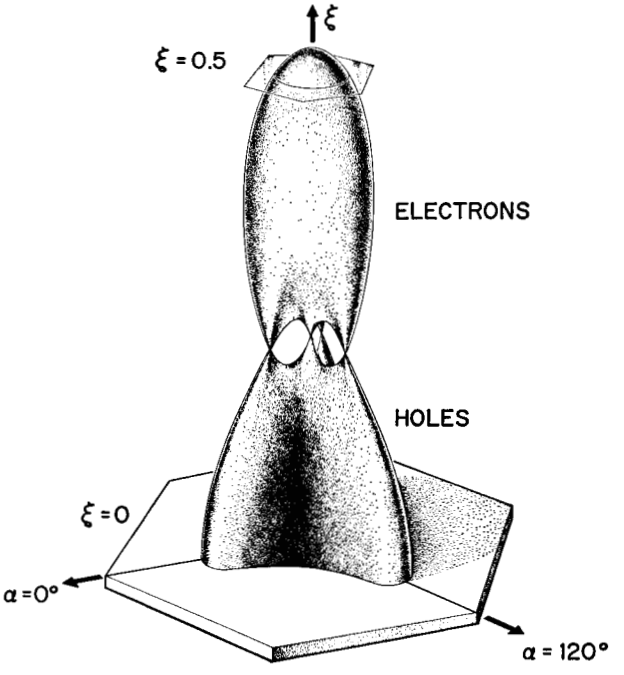

Figure 5 **Model of the graphite Fermi surface.** *To emphasize the trigonal anisotropy, the scale perpendicular to the ξ direction has been expanded by a factor of 5.*

contour for $\xi = 0.140$. The warping eventually becomes so large that by $\xi = 0.209$ the Fermi surface has broken up into four small bits, as is illustrated by the cross section for this value of ξ. As ξ is further increased to $\xi = 0.212$, the three pieces centered at $\sigma \leqq 0.0165$ disappear, and in their place three pieces of electron Fermi surface

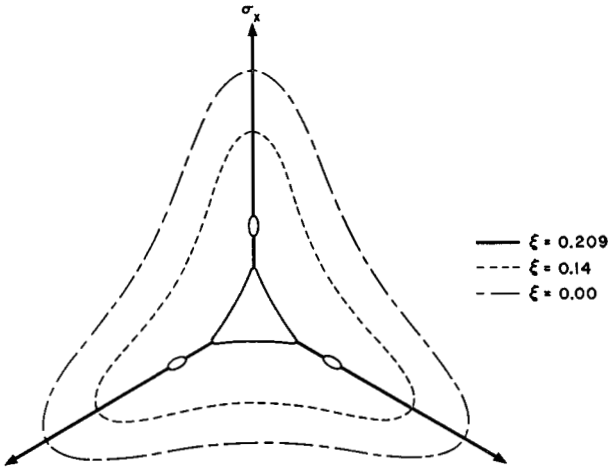

Figure 6 **Scale drawings of selected hole cross sections of the Fermi surface showing the variation from the extremal at $\xi = 0$ to the cross sections near the hole "feet".** *The maximum radius at the extremal cross section is $\sigma = 4.3 \times 10^{-2}$, which is only 1.2% of the distance from the Brillouin zone center to the zone edge.*

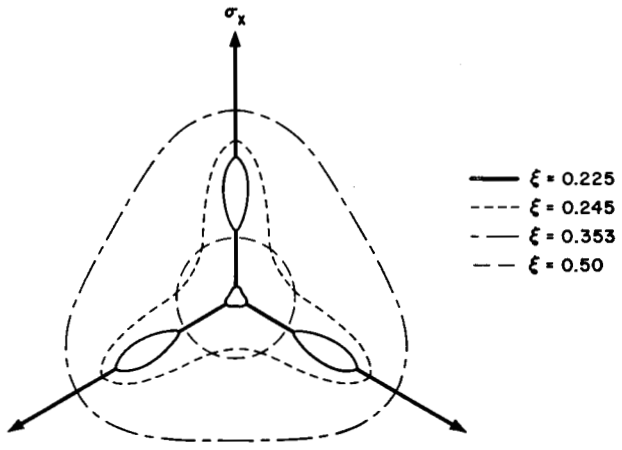

Figure 7 **Scale drawings of selected electron cross sections of the Fermi surface:** *the extremal cross section at $\xi = 0.353$, the warped cross section at $\xi = 0.245$, one of the electron "feet" cross sections at $\xi = 0.225$ and the circular cross section at the Brillouin zone boundary, $\xi = 0.50$. The maximum radius at the extremal cross section is $\sigma = 2.9 \times 10^{-2}$ which is only 0.8% of the distance from the Brillouin zone center to the zone edge.*

appear. The central bit of hole surface at $\xi = 0.212$ remains, decreasing in area until $\xi = 0.222$, where it also disappears and is replaced by a central piece of electron surface. Thus, for the range of ξ values $0.213 < |\xi| < 0.221$, both hole and electron surfaces of small cross sectional area are simultaneously present. A typical cross section for the region of the electron "feet" is shown in Fig. 7 at $\xi = 0.225$. These four bits of Fermi surface increase in size as ξ is further increased and eventually at $\xi = 0.229$ these pieces coalesce. It should be emphasized that the details given here for the behavior of the Fermi surface in the vicinity of the electron and hole "feet" is very sensitive to the exact values of the band parameters. A cross section appropriate to a relatively large electron effective mass is given in Fig. 7 by the warped orbit at $\xi = 0.245$. As ξ increases further, the cross sections become more circular as, for example, the extremal de Haas-van Alphen electron orbit at $\xi = 0.353$ and the circular intersection with the Brillouin zone boundary at $\xi = 0.50$. To summarize these results, plots of the ξ dependence of the Fermi surface cross sectional areas and of the electron and hole cyclotron effective masses are given in Figs. 8 and 9, respectively. Although it is the hole rather than the electron Fermi surface which exhibits by far the larger warping, the effective mass of the holes has a relatively small ξ dependence as compared to that of the electrons. Very large effective masses characterize the boundaries of the hole-electron transition region. Beyond this region

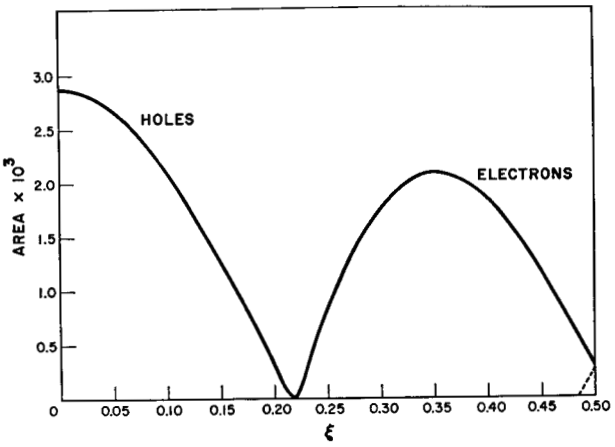

Figure 8 **The dependence of the hole and electron cross sectional areas on ξ.** *The cross sectional areas for the minority electrons near $\xi = 0.50$ are indicated by the dashed line.*

of ξ, an almost linear decrease in the electron effective mass occurs with increasing ξ.

The warping of the cross sections of the Fermi surfaces depends only on the parameter γ_3. Furthermore, the fine details of the hole-electron transition region are especially sensitive to this parameter. The most quantitative determination of γ_3 has been made from an analysis of the

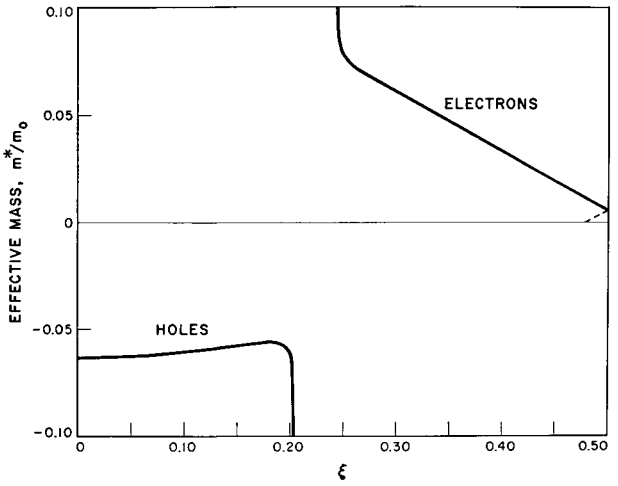

Figure 9 **The dependence of the hole and electron cyclotron effective masses on ξ.** *The effective masses for the minority electrons near $\xi = 0.50$ are indicated by the dashed line.*

magnetoreflection results for interband transitions about point K in the limit of low quantum number. A more precise value of this parameter could be obtained by extending the magnetoreflection experiments to higher magnetic fields, and lower photon energies, and by using samples of higher crystalline perfection. One of the weaknesses of the magnetoreflection experiment is that γ_3 is not determined independently of the other band parameters. One experiment which could determine this parameter more directly is the observation of a de Haas - van Alphen hole or electron period with the magnetic field lying in the basal plane. Such an experiment would be particularly sensitive to the "feet" of the hole-electron transition region. Since the extremal areas for the $\mathbf{H} \perp \mathbf{c}$ configuration are not very pronounced, the intensity of the oscillations is expected to be weak. Soule, McClure, and Smith[9] have observed such oscillations, but with very low intensity. However, their results have not yet been analyzed to yield a quantitative value for γ_3.

References

1. M. S. Dresselhaus and J. G. Mavroides (to be published).
2. R. R. Haering and S. Mrozowski, *Progress in Semiconductors*, John Wiley and Sons, New York, 1960, vol. 5, p. 273. This review article contains a comprehensive list of references to work on the graphite electronic band structure.
3. J. W. McClure, *Phys. Rev.* **108**, 612 (1957).
4. P. Nozières, *Phys. Rev.* **109**, 1510 (1958).
5. C. A. Klein, W. D. Straub and R. J. Diefendorf, *Phys. Rev.* **125**, 468 (1962).
6. The microcrack spacing is difficult to estimate and varies a great deal over the sample dimensions. The 1 μ spacing represents an order of magnitude estimate.
7. J. W. McClure, *Phys. Rev.* **119**, 606 (1960); M. Inoue, *J. Phys. Soc. Japan* **17**, 808 (1962).
8. D. Shoenberg, *Phil. Trans. Roy. Soc.* (London) **245**, 1 (1952); T. G. Berlincourt and M. C. Steele, *Phys. Rev.* **98**, 956 (1955).
9. D. E. Soule, J. W. McClure and L. B. Smith (to be published).
10. J. W. McClure, *J. de Chimie Physique*, **57**, 859 (1960).
11. D. F. Johnston, *Proc. Roy. Soc.* **A227**, 349 (1955).
12. J. W. McClure and Y. Yafet, *Proceedings of the Fifth Conference on Carbon*, Pergamon Press, Inc., Oxford and New York, 1962, p. 22.

Discussion

J. A. Krumhansl: Could you comment on the negative sign of γ_4? Is there a physical reason for this choice of sign?
M. S. Dresselhaus: As far as the magnetoreflection experiment is concerned, it is only the magnitude of γ_4 which enters the analysis. It measures the departure from mirror symmetry for magnetic energy levels in the valence and conduction bands. We have found that the ratio of de Haas - van Alphen hole and electron periods is sensitive to the sign of γ_4. In order to get agreement between the magnetoreflection experiment and these periods we have been forced to take the negative sign. Since γ_4 involves a matrix element of a component of momentum taken between orbitals on two different carbon atoms, there is no physical reason to expect one sign rather than another for γ_4.
P. Grosewald: Does your experiment give evidence for "light" electrons and holes?
Dresselhaus: If the magnetic field is along the *c* direction, the major trigonal direction, our calculations show only two extremal cross sections, one for the usual electron period, one for the usual hole period. These are both associated with relatively light mass carriers.

If you tip the magnetic field out of the *c* direction, you can get different de Haas - van Alphen periods, depending on the exact values of the band parameters. These other periods, however, are short periods and are not associated with low mass carriers.
Grosewald: Have you seen these other periods in your experiment?
Dresselhaus: In our experiment we have not observed any de Haas - van Alphen type periods. We do observe an oscillatory phenomenon which can be interpreted to yield band parameters for graphite. Using these band parameters, we *calculate* the shape of the Fermi surface and *predict* de Haas - van Alphen periods.
C. A. Klein: Since your experiments do *not* provide a value of γ_2, I am wondering how you arrived at the value $\gamma_2 = 0.016$ eV listed in your table.
Dresselhaus: γ_2 is the one parameter that our experiment has not yielded. In principle, our experiment should also determine γ_2, if we went to sufficiently low photon energies and looked at the optical analog of the de Haas - van Alphen effect. We have not done this. I forgot to mention in the talk that the value given in the Table was obtained by borrowing either an electron or a hole period from de Haas - van Alphen measurements of either the diamagnetic susceptibility or the magnetoresistance.
G. Wagoner: The nose of your Fermi-surface rocket (Fig. 5) shows a small overlap in the next zone. You also indicate that you have minority carriers. Would these act like ordinary minority carriers and show a de Haas - van Alphen period?
Dresselhaus: We call these carriers "minority carriers" only because of the notation we have used. These pockets of electrons are formed not by one of the E_3 bands but by the E_1 band and the Fermi energy. In the extended zone scheme, these carriers are outside the first Brillouin zone. There is no energy discontinuity at the zone face, and no de Haas - van Alphen period would be observed for these carriers.